Molecular Biology of the Cell
Vol. 13, 1846–1856, June 2002

The Cytoplasmic Tail of Invariant Chain Regulates Endosome Fusion and Morphology

Tommy W. Nordeng,*†‡ Tone F. Gregers,†‡ Thomas Lasker Kongsvik,† Stéphane Méresse,* Jean-Pierre Gorvel,* Fabrice Jourdan,§ Andrea Motta,§ and Oddmund Bakke†‖

†Division of Molecular Cell Biology, Department of Biology, University of Oslo, 0316 Oslo, Norway; *Centre d'Immunologie de Marseille-Luminy, Centre National de la Recherche Scientifique-INSERM-Univ-Med, 13288 Marseille, Cedex 09, France; and §Istituto di Chimica Biomolecolare del Consiglio Nazionale delle Ricerche, Comprensorio Olivetti, I-80078 Pozzuoli (Napoli), Italy

Submitted October 2, 2001; Revised February 20, 2002; Accepted March 20, 2002
Monitoring Editor: Howard Riezman

The major histocompatibility complex class II associated invariant chain (Ii) has been shown to inhibit endocytic transport and to increase the size of endosomes. We have recently found that this property has a significant impact on antigen processing and presentation. Here, we show in a cell-free endosome fusion assay that expression of Ii can increase fusion after phosphatidylinositol 3-kinase activity is blocked by wortmannin. In live cells wortmannin was also not able to block formation of the Ii-induced enlarged endosomes. The effects of Ii on endosomal transport and morphology depend on elements within the cytoplasmic tail. Data from mutagenesis analysis and nuclear magnetic resonance-based structure calculations of the Ii cytoplasmic tail demonstrate that free negative charges that are not involved in internal salt bridges are essential for both interactions between the tails and for the formation of enlarged endosomes. This correlation indicates that it is interactions between the Ii cytoplasmic tails that are involved in endosome fusion. The combined data from live cells, cell-free assays, and molecular dynamic simulations suggest that Ii molecules on different vesicles can promote endosome docking and fusion and thereby control endosomal traffic of membrane proteins and endosomal content.

INTRODUCTION

Invariant chain (Ii) is a type II transmembrane glycoprotein known to have several important functions in antigen presentation (for a review see Germain, 1994; Nordeng *et al.*, 1998). In the endoplasmic reticulum (ER) Ii trimers transiently associate with major histocompatibility complex (MHC) class II $\alpha\beta$ 10 dimers. MHC class II molecules are transported from the ER to the endocytic pathway where they encounter endocytosed antigens. Two Leu-based–sorting signals in the cytoplasmic tail are independently sufficient for efficient endosomal targeting of Ii (Pieters *et al.*, 1993; Bremnes *et al.*, 1994; Odorizzi *et al.*, 1994). During intracellular transport of $\alpha\beta$-Ii complexes, Ii is sequentially degraded from the luminal side (Blum and Cresswell, 1988). Partially degraded Ii remains trimeric and still associated with MHC class II, suggesting that the luminal region is not required for maintaining the nonameric $\alpha\beta$-Ii complex (Amigorena *et al.*, 1995; Newcomb *et al.*, 1996).

At high levels of expression, Ii has been reported to accumulate in enlarged endosomal compartments in transfected cells (Pieters *et al.*, 1993; Romagnoli *et al.*, 1993). In addition, Ii expression has been shown to cause a delayed endocytic transport of both antigens and membrane proteins in transfected cells (Romagnoli *et al.*, 1993; Gorvel *et al.*, 1995; Gregers, Nordeng, Gilje, Sandlie, and Bakke, unpublished data). These results demonstrate that Ii can modify the structure and function of the endosomal compartment, and this could influence antigen processing and presentation. A morphological study of Ii-induced large endosomal vesicle(s) (ILEV) in a human fibroblast cell line demonstrated that enlarged compartments containing early endosomal markers appeared as single membrane vesicles, whereas those containing late markers were generally filled with internal membranes (Stang and Bakke, 1997). Chimeric proteins consisting of the Ii tail fused to reporter molecules that formed tetramers did not induce vacuolation (Pieters *et al.*, 1993; Bremnes *et al.*, 1994). In addition, Ii constructs unable to trimerize were localized in normal-sized endosomes, showing that the luminal region of Ii was involved in Ii-

Article published online ahead of print. Mol. Biol. Cell 10.1091/mbc.01–10–0478. Article and publication date are at www.molbiolcell.org/cgi/doi/10.1091/mbc.01–10–0478.

‡ The authors have contributed equally to this work.

‖ Corresponding author. E-mail address: oddmund.bakke@bio.uio.no.

Table 1. Ii induced vacuolation

No	Construct	1	2	3	4	5	6	7	8	9								17	Internalization of BU43	ILEV	Tailpiece charge	Free negative charge
1	wt	M	D	D	Q	R	D	L	I	S	N	N	E	Q	L	P	M	L	+	+	−2	Yes
2	Δ_{2-8}	M	.	.	.	.	.	.	.	S	N	N	E	Q	L	P	M	L	+	−		Yes
3	Δ_{2-5}	M	.	.	.	.	D	L	I	S	N	N	E	Q	L	P	M	L	+	−/+	−1	Yes
4	Q4A[a]	M	D	D	**A**	R	D	L	I	S	N	N	E	Q	L	P	M	L	+	+	−2	Yes
5	R5A, D6A[a]	M	D	D	Q	**A**	**A**	L	I	S	N	N	E	Q	L	P	M	L	+	+	−2	Yes
6	L7A[a]	M	D	D	Q	R	D	**A**	I	S	N	N	E	Q	L	P	M	L	+	+	−2	Yes
7	I8A[a]	M	D	D	Q	R	D	L	**A**	S	N	N	E	Q	L	P	M	L	+	+	−2	Yes
8	R5D, D6R	M	D	D	Q	**D**	**R**												+	+	−2	Yes
9	D3R, R5D	M	D	**R**	Q	**D**	D												+	+	−2	Yes
10	Q4D, R5Q, D6R	M	D	D	**D**	**Q**	**R**												+	+	−2	Yes
11	D2A, D3A[a]	M	**A**	**A**	Q	R	D												+	+	0	Yes
12	D2R	M	**R**	D	Q	R	D												+	+	0	Yes
13	D2A, D3E, D6A	M	**A**	**E**	Q	R	**A**												+	+	0	Yes
14	D3R	M	D	**R**	Q	R	D												+	−	0	No
15	D6R	M	D	D	Q	R	**R**												+	−	0	No
16	D3A, D6A	M	D	**A**	Q	R	**A**												+	−	0	No
17	D2A, D3A, D6A	M	**A**	**A**	Q	R	**A**												+	−	+1	No
18	D3R, D6A	M	D	**R**	Q	R	**A**												+	−	+1	No
29	D2R, D6A	M	**R**	D	Q	R	**A**												+	−	+1	No
20	D2A, D3A, D6R	M	**A**	**A**	Q	R	**R**												+	−	+2	No
21	D2R, D3R, D6R	M	**R**	**R**	Q	R	**R**												−	−	+4	No

Summary of Ii constructs used in this study. Whereas alanine substitutions had no effect on ILEV formation, mutations that changed the overall charge of the N-terminus (D(6)→R or D(3)→R) was sufficient to avoid vacuolation. ILEV: large endosomal structures.

[a] Motta *et al.*, 1995.

induced vacuolation (Gedde-Dahl *et al.*, 1997). Nuclear magnetic resonance (NMR) studies of a synthetic Ii tail peptide have shown that it takes up an α-helix (Motta *et al.*, 1995) and that this peptide at high concentration forms a trimeric aggregate (Motta *et al.*, 1997). Together, these data indicate that Ii trimers are formed by interactions both in its cytoplasmic tail and in the luminal domain.

It has previously been reported that ILEV were not formed in cells expressing a mutant Ii construct lacking the 11 N-terminal amino acids (Pieters *et al.*, 1993; Romagnoli *et al.*, 1993), and Pond *et al.* (1995) showed that acidic amino acid residues upstream of the membrane-distal Leu-based–sorting signal were required for endocytic targeting and vacuolation. In this study, we have further investigated the sequence and the structural requirements within the cytoplasmic tail of Ii that are essential for Ii-induced endosomal vacuolation. Using a cell-free system we have also addressed the mechanisms by which Ii is able to regulate size and morphology of endosomes.

MATERIALS AND METHODS

Recombinant cDNA Constructs

The cDNA fragment encoding the p33 form of human Ii (Ii_{wt}) has been described previously (Bakke and Dobberstein, 1990). An overview of mutants used in this study is given in Table 1. The alanine (Ala)-scanned mutants (nos. 4–7 and 11) have been described previously (Motta *et al.*, 1995). Point mutations or deletions in the cytoplasmic tail of Ii were introduced by polymerase chain reaction (PCR) mutagenesis using Ii_{in} in the expression vector pSV51L (Bakke and Dobberstein, 1990) as template. The forward primers contained the point mutations or deletion and a Kozak translation initiation sequence for proper initiation of translation (Kozak, 1987). The PCR reactions were performed using Vent DNA polymerase (New England Biolabs, Beverly, MA) for primer extension. The final PCR products were cloned into pcDNA3 (Invitrogen, Carlsbad, CA). All mutants were verified by sequencing.

Ii_{wt} and Ii_{D6R} in the heavy metal-inducible expression vector pMEP4 (Invitrogen) has been described (Nordeng and Bakke, 1999). The C-terminal endosome-binding domain of early endosomal antigen 1 fused to green fluorescent protein (EEA1-GFP, McBride *et al.*, 1999) was a gift from Dr. H. Stenmark (Oslo, Norway).

Cell Culture

Madin-Darby canine kidney strain II (MDCK) and COS-1 cells were grown in complete medium: DMEM (Bio Whittaker, Walkersville, MD) supplemented with 9% fetal calf serum (Integro, Zaandam, Holland), 2 mM glutamine 25 U/ml penicillin, and 25 μg/ml streptomycin (all from Bio Whittaker) in 6% CO_2 in a 37°C incubator.

Antibodies and Ligands

The high production in serum-free medium hybridoma BU45-HPSF1 was kindly provided by Dr. S. Buus (Copenhagen, Denmark) and produces the mouse mAb BU45, which recognizes the luminal C-terminal part of human Ii (Wraight *et al.*, 1990). The hybridoma was grown in protein-free hybridoma medium II supplemented with 100 U/ml penicillin and 100 μg/ml streptomycin (all purchased from Life Technologies, Paisly, Scotland). BU43 is a mouse immunoglobulin (Ig) M mAb specific for the luminal C-terminal part of human Ii (Binding Site, Birmingham, UK), and the mouse mAb VicY1 recognizes the N terminus of the Ii tail (Quaranta *et al.*, 1984) and was a gift from Dr. W. Kapp (Vienna, Austria). Goat anti-mouse antibody coupled to Alexa 488 was obtained from Mo-

lecular Probes (Leiden, The Netherlands). Texas Red (TR)-conjugated goat anti-mouse IgM antibody was from the Southern Biotechnology Association, Inc. (Birmingham, AL).

Transfections

COS cells were transiently transfected by the DEAE-dextran method essentially as described by Huylebroeck *et al.* (1988).

MDCK cells stably transfected with Ii_{wt} and Ii_{D6R} have been described (Nordeng and Bakke, 1999; Gregers, Nordeng, Gilje, Saudlie, and Bakke, unpublished data). MDCK cells were transfected with EEA1-GFP by the DNA-calcium phosphate procedure, yielding stable clones as described elsewhere (Wigler *et al.*, 1979). Clones expressing moderate levels of EEA1-GFP were chosen to avoid interference with the endosomal fusion machinery (McBride *et al.*, 1999). Resistant clones were selected in the presence of 500 μg/ml Geneticin (Duchefa, Haarlem, The Netherlands). Approximately 100% positive clones expressing EEA1-GFP were then double-transfected with Ii and selected with 300 μg/ml hygromycin B. Resistant clones were induced with 25 μM $CdCl_2$ for 16 h to induce Ii expression. Double-positive clones were identified by immunofluorescence microscopy.

Immunofluorescence Confocal and Video Microscopy

Transfected cells were grown on glass coverslips and allowed to internalize BU43 for 1 h and then fixed with 3% paraformaldehyde. Fixed cells were incubated for 30 min at room temperature with appropriate antibodies diluted in PBS containing 1% sapponin, washed three times with PBS, and incubated for 30 min with goat anti-mouse Alexa 488 antibodies or goat anti-mouse IgM-Texas Red diluted in PBS/1% sapponin to detect bound primary antibody. The coverslips were then washed and mounted in Fluoromount G (Southern Biotechnology Associates, Birmingham, AL). Confocal images were acquired with a Leica TCS-NT digital scanning confocal microscope (Leica Wetzlar, Germany) equipped with a 60/1.2 water immersion objective. Alexa 488 was excited with the 488 line of a krypton-argon laser and imaged with 515–540 bandpass filters, whereas Texas-Red was excited with the 568 line and imaged with long-pass 590 filters. The images were processed for presentation by Photoshop (Adobe Systems, Mountain View, CA). For quantification of ILEV formation, 25 different images per experiment were studied, and vesicles with diameters larger than 1 μm were defined as ILEV. The fraction of cells containing ILEV, the average number of ILEV per cell, and the average size of ILEV were quantified.

Metabolic Labeling, Immunoprecipitation, and Endo H Treatment

COS cells in 35-mm wells were labeled 2 d after transfection, and stably transfected MDCK cells grown in 35-mm wells were grown to ~75% confluency in full medium supplemented with various concentrations of $CdCl_2$. The cells were then starved in Cys/Met-free DMEM for 45 min at 37°C before labeling in the same medium containing 100 μCi/ml ^{35}Cys/^{35}Met for another 30 min. After labeling, the cells were placed on ice, washed three times in ice-cold PBS, and lysed in ice-cold lysis buffer (50 mM Tris-HCl, pH 7.5, 150 mM NaCl, 1% Nonidet P-40) containing a cocktail of protease inhibitors (4 μg/ml phenylmethylsulfonyl fluoride, 2 μg/ml antipain, 2 μg/ml leupeptin, and 1 μg/ml pepstatin A) for 20 min. The lysate was centrifuged at 10,000 $\times$ *g* for 10 min at 4°C to remove the cell nuclei and cellular debris, and the supernatant was used directly for immunoprecipitation. Ii proteins were precipitated from the supernatant by addition of BU45 for 1 h at 4°C. Dynabeads (0.25 mg)-sheep anti-mouse IgG (Dynal, Oslo, Norway) were then added for a further incubation for 1 h. The beads-antigen complexes were collected using a Dynal magnetic particle concentrator and washed twice with PBS containing 1% Nonidet P-40. Endo H digestion was performed by resuspending the beads in 0.1 M phosphate buffer (pH 5.5) containing a cocktail of protease inhibitors as described above. The samples were split in two and incubated for 3 h at room temperature with or without Endo H (Boehringer-Mannheim, Mannheim, Germany). After incubation, the proteins were eluted from the beads by incubation in gel-loading buffer (50 mM Tris-HCl, pH 6.8, 2% SDS, 10% glycerol, and 0.1% bromphenol blue) at 95°C for 3 min.

Nonreducing gel electrophoresis was performed in a 12% SDS-polyacrylamide gel with a 5% stacking gel, prepared as described by Laemmli (1970). The gels were fixed in 10% acetic acid-30% methanol, and the radioactive signal was amplified using Amplify solution (Amersham Pharmacia Biotech, Piscataway, NJ). The bands were detected with the Molecular Imaging Screen CS (Bio-Rad, Hercules, CA) and analyzed with a Bio-Rad GS-250 Phosphor Imager. The intensity of each band was quantified by the Molecular Analyst 2.0.1 software (Bio-Rad). The amount of Ii protein was quantified and related to the total amount of radiolabeled protein in the lysate, giving the relative Ii protein expression.

NMR Spectroscopy

NMR spectra were recorded on a DRX-500 spectrometer (Bruker, Newark, DE) equipped with a triple resonance probe head and pulsed field gradients. Proton chemical shift assignments were performed using conventional two-dimensional experiments as described in Motta *et al.*, 1997. Data processing was performed using Aurelia 2.0 software (Bruker Analytic GMBH, Reinstetten, Germany) running on Silicon Graphics computers (Mountain View, CA).

Structure Calculations

Model building and preliminary calculations were performed on a United Atom (UA) model (Weiner *et al.*, 1984) with the Sybyl 6.5 package (Tripos, St. Louis, MO). The solvation effects were roughly included using a distance-dependent dielectric constant $\epsilon = r$. In the UA model, distance restraints, as previously derived from NMR spectra of the wild-type 27-amino acid cytosolic Ii tail, were included as the C-C or C-N distance increasing the upper limits calculated for interproton distances of 1 Å. Semiparabolic penalty functions were used with force constants in energy minimization (EM) and room temperature molecular dynamics (MD) simulations of 5 kcal mol^{-1} rad^{-2} for dihedral restraints and 5 kcal mol^{-1} $Å^{-2}$ for distance restraints. In simulated annealing (SA) and preliminary MD runs, a time step of 1 fs, with no restraint on bond length applied, was used. SA calculations were performed with different lengths (from 10–250 ps), temperature (maximum values from 500–800 K, applied for 25–75% of the total time, cooling rates from 1–5 K ps^{-1}), and restraint force constant time profiles. After analysis of energy and violations, the best 40 structures were energy minimized, solvated in a periodic box of 5120 methanol molecules, and subjected to a 500-ps run of restrained MD simulations, followed by 1 ns of unrestrained MD run.

EM and MD simulations with solvent were performed with the Sander module of the Amber 4.1 package using the Amber/OPLS force field (Jorgensen, 1986; Jorgensen and Tirado-Rives, 1988). A time step of 2 fs, with rigid restraining of all bond lengths (SHAKE algorithm, Ryckaert *et al.*, 1977) and periodic boundary conditions were applied. All MD simulations were performed in the isothermal-isobaric ensemble (300 K, 1 atm), with a solvent box that initially extended 8 Å from the most external solute atom on each side of the box. The final analyses were performed with specific modules of the Amber 4.1, Sybyl 6.5, and Molmol (Koradi *et al.*, 1996) packages. Molecular structures have been drawn with Molmol and rendered with the POV-ray software.

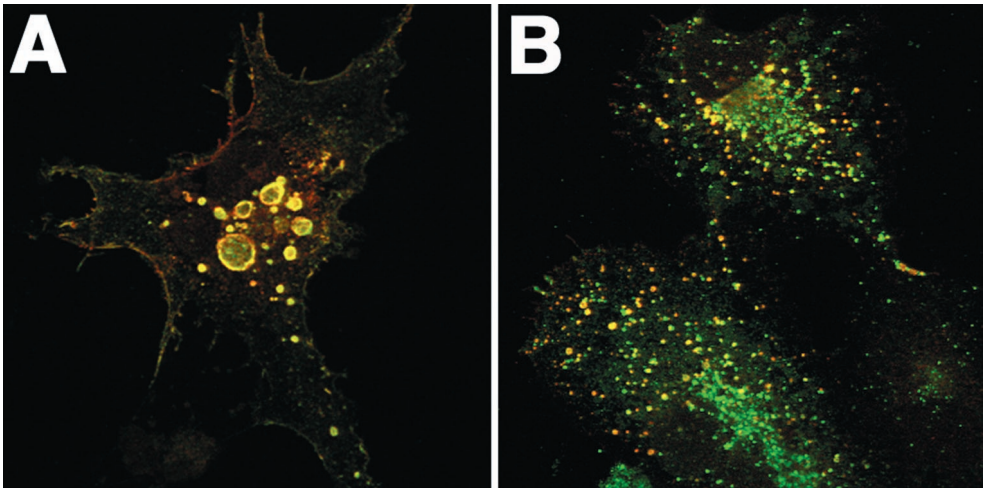

Figure 1. Ii-induced vacuolation. COS cells were transiently transfected with Ii_{wt} (A) or an Ii construct with an Asp residue in the cytoplasmic tail replaced with an Arg, Ii_{D6R} (B). The cells were incubated with an antibody against the luminal domain of Ii (BU43, red channel) for 1 h at 37°C, fixed, and labeled with an antibody against the cytoplasmic domain of Ii (VicY1, green channel) to identify total Ii protein. Bar, 10 μm.

Quantification of Cell-free Fusion of Endocytic Vesicles

Cell-free endosome fusion was quantified as previously described (Gruenberg *et al.*, 1989; Bomsel *et al.*, 1990; Gorvel *et al.*, 1991). Briefly, 80% confluent cells were incubated for 30 min with 1.8 mg/ml biotinylated horseradish peroxidase (bHRP) or 3.6 mg/ml avidin. After washing with PBS/bovine serum albumin, cells were homogenized in homogenization buffer (250 mM sucrose, 3 mM immidazole, pH 7.4) by six passes through a 1.25″× 22-G needle, and postnuclear supernatants were prepared. Aliquots (50 μl) of the two postnuclear supernatants were combined in the presence of 50 μl of rat liver cytosol (10 mg/ml protein), adjusted to 12.5 mM HEPES (pH 7.4), 1.5 mM MgOAc, 3 mM imidazole (pH 7.4), 1 mM dithiothreitol, 50 mM KOAc, and complemented with 8 μl of an ATP-generating system (1:1:1 mixture of 100 mM ATP brought to pH 7.0 with KOH, 800 mM creatine phosphate, and 4 mg/ml creatine kinase) and 8 μl of a 1-mg/ml biotin-insulin stock solution as a quenching agent. To deplete ATP, 1.6 μl of apyrase (1.200 U/ml) replaced the ATP-generating system. The fusion reaction was carried out for 45 min at 37°C, eventually in the presence of 1 mM *N*-ethylmaleimide (NEM) or 100 nM wortmannin, before Triton X-100 solubilization. Avidin was then immunoprecipitated, and the associated HRP was quantified by colorometry.

Materials

All materials, unless specified otherwise, were purchased from Sigma (St. Louis, MO).

RESULTS

ILEV Formation Depends on the Ii Cytoplasmic Tail N Terminus but Not on Specific Amino Acid Residues

Transient expression of Ii in transfected COS cells causes the formation of enlarged endosomes (Figure 1). We have used this phenotype, defined as spheres with a diameter >1 μm, as an assay to study the structural requirements for vacuolation. The N-terminal 11 first amino acids of the Ii cytoplasmic tail has previously been shown to be required for ILEV formation (Pieters *et al.*, 1993). A panel of Ii constructs with mutated cytoplasmic tails were therefore transiently expressed in transfected COS cells and subjected to immunofluorescence microscopy (Table 1). To identify the minimal region of the Ii cytoplasmic tail required for vacuolation, we first expressed two additional deletion mutants. $Ii_{\Delta 2-8}$ (no. 2) did not induce vacuolation, whereas expression of $Ii_{\Delta 2-5}$ (no. 3) did, but less extensively than Ii_{wt}. This indicated that information for vacuolation was contained within the six first residues in the cytoplasmic tail of Ii, denoted as the Ii tailpiece. To investigate whether single amino acids within this region were required for vacuolation, we substituted all amino acids in positions 2–8 with Ala residues. Immunofluorescence and phase contrast microscopy analysis showed that all mutants induced vacuolation to similar extents as Ii_{wt} (Table 1, nos. 4–7 and 11).

From a previous study it was reported that the sorting signal in the N-terminal region of the cytoplasmic tail, Leu^7Ile^8, was not required for ILEV formation as long as the second signal was kept intact (Bremnes *et al.*, 1994). The second Leu signal may also be replaced with tyrosine-based endosomal sorting signals (from the transferrin receptor or TGN 38) without affecting vacuolation, showing that vacuolation is not dependent on a specific endosomal sorting signal (Bremnes and Bakke, unpublished data).

Ii harbors four charged amino acids within the N-terminal tailpiece: three aspartic (Asp) residues and one arginine (Arg) giving a net negative charge in this region of −2. In addition, previous studies of Ii trafficking (Pond *et al.*, 1995) have demonstrated a role for charged amino acids within the tailpiece of Ii. As noted in Table 1, Ala substitutions, except for construct 11, did not change the overall charge of the tailpiece and all still induced ILEV formation. The Δ 2–5 truncation, although presenting a single negative charge in the tail, also formed ILEV. These data prompted us to ask whether the charge distribution rather than the specific amino acid sequence would determine ILEV formation. We studied the role of the charged residues by introducing amino acids that altered the overall charge distribution in the tailpiece or by inverting charges at specific positions. We observed that when the total charge of the N-terminal tailpiece was negative (nos. 3–10) we always observed vacuolation. In contrast, a total positive charge (nos. 17–21) always prevented ILEV formation. However, when the tailpiece had

a neutral charge, some constructs formed ILEV (nos. 11–13), whereas others did not (nos. 14–16). This encouraged us to study in more detail the requirement for negative charges at specific sites. Changing Asp^2 to Arg (Ii_{D2R}, no. 12) caused ILEV formation. In contrast, the Asp^3 to Arg (construct 14) and Asp^6 to Arg (no. 15) substitutions were sufficient to prevent vacuolation (Table 1; Figure 1). Similar results were obtained when Lys was introduced in position 3 or 6, suggesting that positive charges in these positions prevented vacuolation. Likewise, when the Asp in position 3 or 6 were replaced with another acidic residue, Gla, ILEV still formed (data not shown), indicating that the Asp residue per se was not required, but rather the presence of a negative charge appeared to be necessary. When both positions 3 and 6 were exchanged simultaneously for Ala residues (no. 16), vacuolation did not occur, indicating that Asp^2 alone was not sufficient for vacuolation.

Although endosomal distribution of the constructs was confirmed by immunofluorescence microscopy (Figure 1), the inability of some mutants to form ILEV could in principle be due to inefficient transport to endosomes. Hence, transfected COS cells were subjected to metabolic labeling, immunoprecipitation, and Endo H treatment. Cells expressing Ii_{wt}, Ii_{D3R}, and Ii_{D6R} all gained Endo H resistance, indicating that a fraction of the proteins was successfully transported out of the ER to the TGN (Figure 2). However, a control construct, $Ii_{D2R/D3R/D6R}$ (no. 21) containing two double-Arg ER retention motifs (Schutze *et al.*, 1994), was sensitive to Endo H, indicating that most of this construct did not reach the TGN. These data demonstrate that, except for $Ii_{D2R/D3R/D6R}$, mutations in the cytoplasmic tailpiece did not significantly affect the intracellular distribution of the resulting Ii constructs.

Predicting Vacuolation: The Importance of Available Negative Charges Not Involved in (i, i ± 3) Salt Bridges within the Ii Tailpiece

MD simulations of some of the above constructs helped to explain the mutation data. For the calculations we relied on the structure found for the wild-type 27-amino acid peptide. We have reported that an Ii tail peptide takes up an α-helix that spans the region from Asp^3 to Leu^{17} with a kink on Pro^{15} (Figure 3A; Motta *et al.*, 1995) and that it can form a triple-stranded α-helical bundle (Figure 3B) at high concentration (Motta *et al.*, 1995). Constructs with internal Ala substitution induced vacuolation (Table 1) without affecting the helix and the -2 tailpiece charge. Figure 3C shows MD simulations of the 27-amino acid peptide corresponding to construct 6 (Ii_{L7A}), for which a helix is observed. Analogously, the structure found for constructs 4 and 7 is helical. For construct 5 ($Ii_{R5A,D6A}$), Ala substitution cancels the wild-type Asp^3-Asp^6–capping box (Forood *et al.*, 1993), thus shortening the helix (Figure 3D). However, the tailpiece charge and the ILEV formation are not altered (Table 1), and the same is true for construct 11 ($Ii_{D2A,D3A}$, Figure 3E), although the tailpiece charge is now 0. Construct 14 (Ii_{D3R}) is very interesting because it bears a neutral tail, for which vacuolation is not observed (Table 1), but MD simulations indicate the presence of a helix (Figure 3F). Finally, although vacuolation is not observed, a short helix, similar to that observed for construct 5 (Figure 3D), was predicted for constructs 17–21, all showing a positive tailpiece.

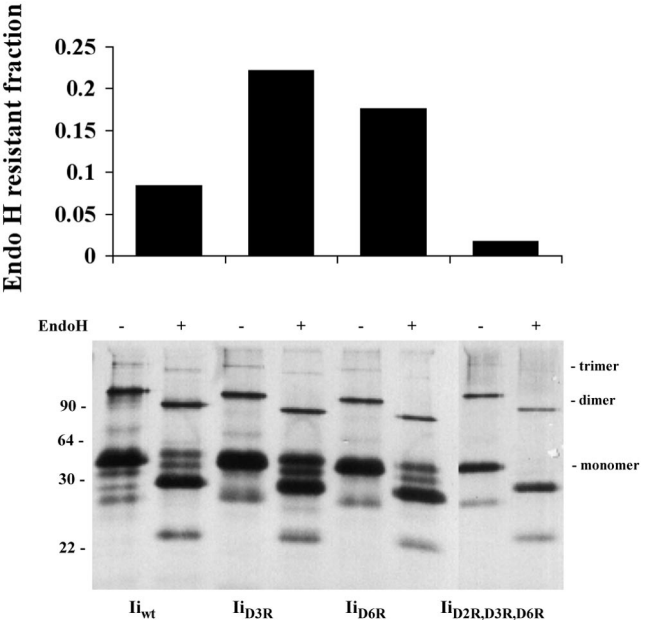

Figure 2. Endo H resistance of different Ii constructs. Transiently transfected COS cells expressing different Ii mutants were metabolically labeled, and Ii proteins were immunoprecipitated with BU45 and incubated with or without Endo H. The samples were subjected to SDS-PAGE, and the Endo H resistant fractions were quantified as described in MATERIALS AND METHODS. The values presented in the graph are from a representative experiment.

The above data rule out that vacuolation is linked to the helix, because its different length does not affect ILEV formation. What appears to be relevant is the presence of an available negative charge at either position 2, 3, or 6 not engaged in an i ± 3 electrostatic interaction. The electrostatic interactions observed in the Ii_{wt} and constructs with a neutral tailpiece are reported in Table 2. It is interesting to observe that for constructs 14–16 all the negative charges within the tail are engaged in (i, i ± 3) salt bridges with Arg, whereas in constructs 11–13 at least one negative charge is available for further interactions (Table 2). Accordingly, whereas the former constructs do not vacuolate, the latter do form large vesicles.

It could be argued that the above electrostatic interactions are essentially due to restraints imposed on the N terminus by the presence of a helix. We therefore studied the solution structure of hexapeptides corresponding to constructs 14, 15, and 16 (MDRQRD-NH_2, MDDQRR-NH_2, and MDAQRA-NH_2, respectively) in their amidated form to avoid the electrostatic contribution of the C terminus. NMR spectra indicated the presence of strong nuclear Overhauser effects between backbone amide protons of residues 3–4 and residues 4–5, as well as an effect between the α proton of Asp^2 and the amide proton of Arg^5 in all hexapeptides. They strongly suggest the presence of a type I β-turn comprising Asp^2-Arg^5 for all of them. Refinement of the structure by MD simulations highlighted the presence of a hydrogen bond between the Asp^2 side chain and the amide proton of Gln^4 backbone NH, as well as with the side chain of Arg^5. Therefore, the isolated neutral tailpiece assumes a confor-

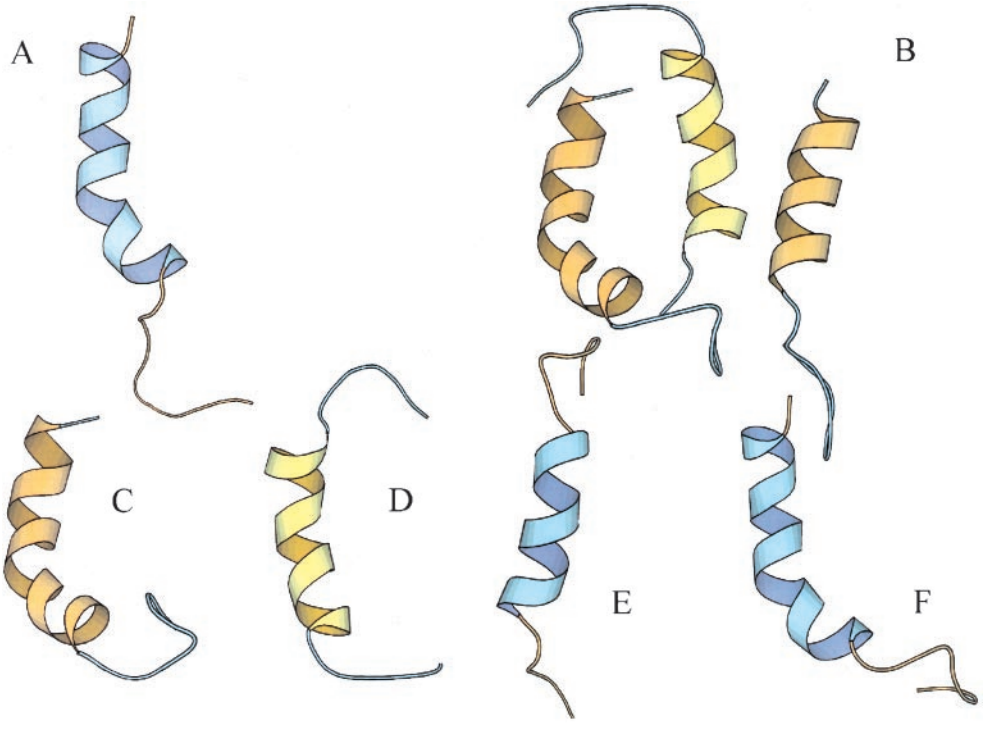

Figure 3. MD calculations of Ii cytoplasmic tails. Structures of different mutants as derived from 1-ns unrestrained molecular dynamics calculations of peptides in methanol solvent. (A) Ii_{wt}; (B) triple-stranded α-helical bundle of the Ii_{wt} peptide; (C) construct 6, Ii_{L7A}; (D) construct 5, $Ii_{R5A,\ D6A}$; (E) construct 11, $Ii_{D2A,\ D3A}$; (F) construct 14, Ii_{D3A}. Large ribbons and tubes correspond to helical regions and other conformations, respectively. Structures have been drawn with Molmol.

mation that favors the network of electrostatic interactions present in wild-type Ii, independently of the secondary structure that follows. Altogether, the mutagenesis analysis and MD data show that ILEV formation does not depend on specific amino acids but on free negative charges within the Ii cytoplasmic tail, which are available for interactions required for vacuolation.

Vacuolation Depends on the Ii Expression Level

Ii-induced endosomal vacuolation would require that a substantial amount of Ii is transported to endosomes. We have shown above that the intracellular routing of Ii and the Ii constructs could not account for the differences in the ability to induce ILEV. However, it was also necessary to study in more detail ILEV formation in response to the expression level. To this end, MDCK cells were stably transfected with Ii_{wt} or Ii_{D6R} under the control of an inducible metallothionein promoter. Using this system, we previously demonstrated that protein expression was proportional to the concentration of $CdCl_2$ in the 0–40 μM range (Nordeng and Bakke, 1999). The MDCK cells were incubated with various concentrations of $CdCl_2$ overnight, metabolically labeled, and lysed, and Ii proteins were immunoprecipitated and subjected to SDS-PAGE. The amount of protein immunoprecipitated from the lysate was quantified as described in MATERIALS AND METHODS, and the protein expression level was related to the $CdCl_2$ concentration. Cells were also grown on coverslips and incubated with the same concentration of $CdCl_2$ as above and labeled for Ii. Figure 4 shows that the fraction of cells containing ILEV, the average number of ILEVs per cell, as well as the average size of ILEV increased with augmented Ii_{wt} expression. In contrast, endosomes were normal-sized when Ii_{D6R} was expressed at high levels similar to Ii_{wt}. This shows that one specific positively charged amino acid in the Ii cytoplasmic tail is sufficient to impair the ability of Ii to induce ILEV.

Ii-induced Endosome Vacuolation and Fusion Is Insensitive to Wortmannin

The giant size of the ILEV depends on membrane supply, most likely obtained by endosome fusion, and we have found that ILEV are generated from a population of early endosomes (Bakke and Nordeng, Nordeng, Gregers, Kongsvik, Méresse, Gorvel, Jourdan, Motta, and Bakke, unpublished data). To study the role of early endosome fusion for ILEV formation, CV1 cells were double-transfected with Ii_{wt} and $rab5_{Ile133}$, a dominant negative mutant that inhibits early endosome fusion (Gorvel *et al.*, 1991). Whereas the normal phenotype of $rab5_{Ile133}$ is early endosome fragmentation, we found by confocal microscopy that ILEV were still formed in double-transfected cells, and conversely, Ii_{D6R} did not inhibit vacuolation induced by the constitutively active $rab5_{L79}$ mutant. This suggested that the Ii-induced vacuolation was uncoupled from the rab5-regulated endosome fusion. To study this further, we used wortmannin, a specific inhibitor of phosphatidylinositol 3 (PI3)-kinase that has been reported to block fusion of early endosomes in cell-free assays (Jones and Clague, 1995; Jones *et al.*, 1998). We first studied Ii-induced vacuolation in the presence of wortmannin in live MDCK cells expressing inducible Ii_{wt} or Ii_{D6R}. We chose to use Ii_{D6R} as a model for cells with normal-sized vesicles, because this mutant has been shown not to interfere with the transport capacity of Ii itself and MHC class II

Table 2. Electrostatic interactions within the cytoplasmic tailpiece of wild type Ii and constructs with neutral tailpiece as derived from MD simulations

	Position		
Construct	2	3	6
1 wt	Asp^3	Asp^2	Asp^3
	*Arg^5	Gln^4	Gln^4
		Asp^6	Ser^9
			Asn^{10}
11 D2A, D3A			Gln^4
			Ser^9
			Asn^{10}
			Asn^{11}
12 D2R	Gln^4	Gln^4	Asp^3
		Asp^6	Gln^4
			Ser^9
			Asn^{10}
13 D2A, D3E, D6A		Gln^4	
14 D3R	Gln^4	Gln^4	*Arg^3
	*Arg^5	*Asp^6	Gln^4
			Ser^9
15 D6R	Asp^3	Gln^4	*Asp^3
	Gln^4	*Arg^6	Gln^4
	*Arg^5		Ser^9
16 D3A, D6A	Gln^4		
	*Arg^5		

For the primary structure of constructs, refer to Table 1. i, i ± 3 interactions with residues 2, 3, and 6 are marked with an asterisk.

(Gregers, Nordeng, Gilje, Sandlie, and Bakke, unpublished data). Fresh wortmannin was added to the cells every 1 h, but it had no detectable effect on the formation of ILEV (Figure 5A). Moreover, wortmannin had no observable impact on preformed ILEV even after 8 h of incubation (Figure 5B). The effect of wortmannin on EEA1 distribtution was studied in cells coexpressing EEA1-GFP. EEA1-GFP was bound to endosomes throughout the cytoplasm (Figure 5C), but within 5 min after addition of 100 nM wortmannin, EEA1-GFP was relocated to the cytoplasm, and little visible staining of endosomes could be detected (Figure 5D). Because wortmannin blocks binding of EEA1 rather than inducing a release, this indicates that the turnover of EEA1 on the early endosome membrane is fast, <5 min. Together, the data show that ILEV formation does not depend on recruitment of rab5 and EEA1 onto endosomal membranes.

These results prompted us to ask whether Ii has a role in endosome fusion, and this was addressed using a cell-free endosome fusion assay. Cells were incubated with Cd^{2+} for 3.5 h to obtain mostly normal-sized Ii-positive endosomes. bHRP or avidin was then endocytosed for 30 min to label both early and late endosomes. A cell-free endosome fusion assay was then carried out as described in MATERIALS AND METHODS. Endosome fusion was dependent on an ATP-regenerating system both in the presence and absence of Ii expression and was inhibited by NEM (Figure 6). The data also show that endosomes from cells expressing Ii_{wt} fused with ~20% higher efficiency than endosomes from nontransfected cells and cells transfected with Ii_{D6R} (Figure 6). When wortmannin was added to the fusion mixture, the fusion efficiency was reduced to 50% in both control cells and cells transfected with Ii_{D6R}, whereas, the fusion efficiency was reduced by only 10% using endosomes from Ii_{wt}-transfected cells. When Ii_{wt} endosomes were fused with Ii_{D6R} endosomes in the presence of wortmannin, there was a 35% reduction in efficiency. The data show that Ii can complement for wortmannin in endosome fusion. The above data thus indicate that Ii is able to increase endosome fusion via a mechanism, which is able to complement for fusion processes inhibited by wortmannin.

DISCUSSION

The Ii-induced endosomal vacuolation and retention observed in transfected cells hints for a previously undescribed cell biological function of Ii. In this study we have attempted to elucidate the structural requirements for and the mechanism behind this effect of Ii expression. We have

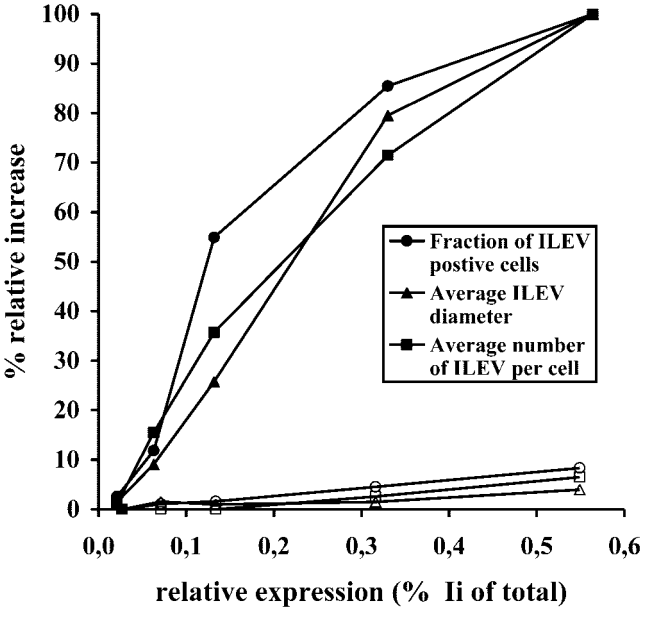

Figure 4. ILEV formation as a function of the Ii expression level. MDCK cell expressing inducible Ii_{wt} or Ii_{D6R} were incubated overnight with 0, 5, 10, 20, and 40 μCl_2, metabolically labeled, and lysed, and Ii proteins were immunoprecipitated by the anti-Ii antibody BU45, before subjected to an SDS-PAGE. The amount of Ii protein was quantified and related to the total amount of radiolabeled protein in the lysate, giving the relative Ii protein expression. Cells grown on coverslips were incubated with the same concentrations of $CdCl_2$ as above and analyzed by immunofluorescence microscopy. Images were acquired by a random procedure, and ILEV were identified on 25 different images per experiment, with three to five cells per image, as vesicles with diameter >1 μm. At the highest expression level, the fraction of cells containing ILEV (circles) was 0.76, the average number of ILEV per cell was 2.77 (squares), and the average size of the ILEV was 2.36 μm (triangles). These numbers were related to the values obtained with lower expression levels, and the percentage relative increase was expressed as a function of the relative Ii expression level as determined in a typical experiment. Closed symbols, Ii_{wt}; open symbols, Ii_{D6R}

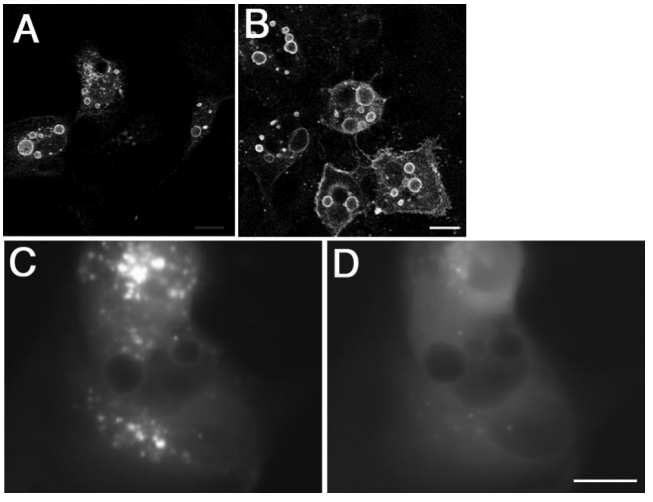

Figure 5. Effects of wortmannin on ILEV formation and EEA1-GFP distribution. MDCK cells stably transfected with Ii and EEA1-GFP were induced to express Ii for 5 h (A) or 8 h (B–D). Wortmannin (100 nM), added from fresh stock every 1 h, was included in the medium containing 25 μM $CdCl_2$ during Ii induction (A) or for 8 h after Ii induction (B) before the cells were fixed and labeled with anti-Ii antibody BU45. Live cells coexpressing EEA1-GFP (C) were incubated with 100 nm Wortmannin and monitored by video microscopy. (D) The situation after 5 min. Bar, 10 μm.

shown that the negative charges provided by acidic residues in the cytoplasmic tail of Ii are a prerequisite for ILEV formation. Acidic residues upstream of the membrane-distal Leu-based sorting signal of Ii have previously been shown to be necessary for this motif to work efficiently in endosomal transport (Motta *et al.*, 1995; Pond *et al.*, 1995; Simonsen *et al.*, 1998a). However, the Leu-based motif per se is not required for vacuolation, because Ii constructs with the $Leu^{7}Ile^{8}$-based motif inactivated and the $Met^{16}Leu^{17}$-based signal replaced by Tyr-based motifs were also vacuologenic (Nordeng, Gregers, Kongsvik, Méresse, Gorvel, Jourdan, Motta, and Bakke, unpublished data).

Pond *et al.* (1995) found that when the eight N-terminal residues of the Ii tail, comprising the $Leu^{7}Ile^{8}$ signal and the upstream acidic residues, were replaced by the corresponding region from the lysosomal integral membrane protein II, M6PR, or CD3γ, vacuolation still occurred. These replacements did not change the overall negative charge of the tailpiece. However, when the tail was replaced with the corresponding region of CD4, which lacks an overall negative charge, vacuolation was not observed (Pond *et al.*, 1995). We substituted the Asp residues in position 3 or 6 with Arg in full-length Ii, changing the net charge in the tailpiece from -2 to zero, and we found that these single mutations were sufficient to avoid vacuolation. Intracellular trafficking of the mutants and wild-type Ii was compared by immunofluorescence microscopy and by quantification of the fractions of newly synthesized proteins that gained Endo H resistance, and there is no indication from the results that the inability of the mutants to form ILEV was due to impaired transport to the endocytic pathway. Moreover, structural data suggest that vacuolation can be interpreted in terms of (i, i $\pm$ 3) electrostatic interactions present in the Ii tailpiece. This was

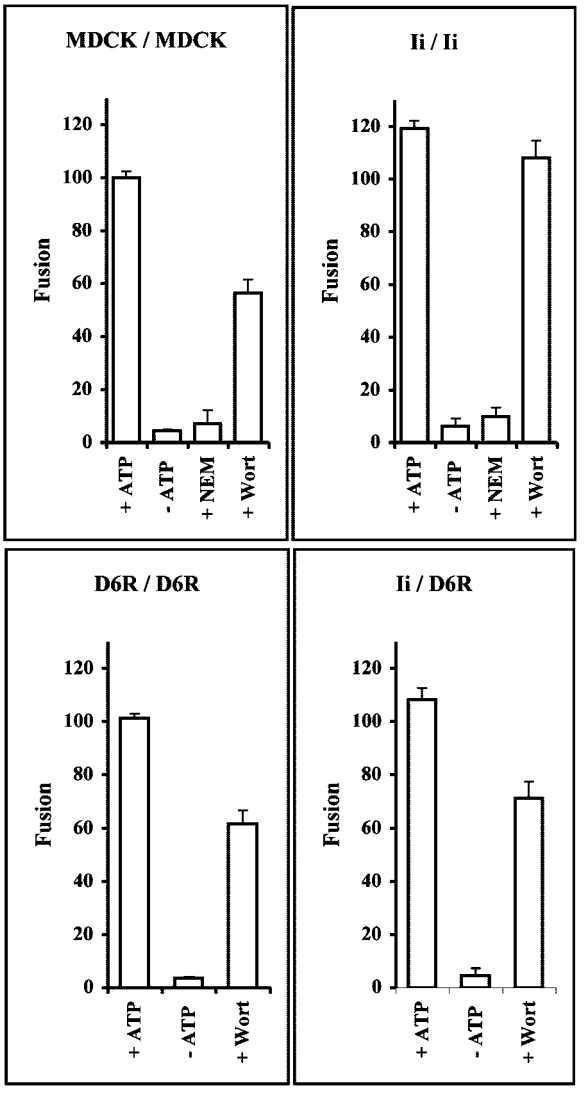

Figure 6. Cell-free endosome fusion. Nontransfected MDCK cells, or stably transfected with Ii_{wt} or Ii_{D6R}, were incubated with 25 μM $CdCl_2$ for 3.5 h. Two separate postnuclear supernatants were prepared after separate 30 -min internalizations either of bHRP or avidin from the medium. In the cell-free assay, the two fractions were mixed with 10 mg/ml cytosol at 4°C. The mixture compositions are indicated. Fusion was initiated by raising the temperature in the presence of an ATP-regenerating system. After 45 min of incubation at 37°C, the mixture was returned to 4°C and solubilized in detergents, and the avidin-bHRP complexes formed during fusion were detected by immunoprecipitation with anti-avidin antibodies. Fusion efficiency was quantified by measuring the enzymatic activity of bHRP. +ATP, the fusion reaction was carried out in the presence of an ATP-regenerating system. −ATP, the ATP-regenerating system was replaced with a depleting system. +Wortmannin (Wort), 100 nM wortmannin was present in the assay. +NEM, 1 mM NEM was present in the assay. The results, representing three experiments performed in duplicate, are presented as percentages of the efficiency obtained with nontransfected MDCK cells, corrected for the fraction of transfected cells as estimated by fluorescence microscopy. Error bars, 1 SE.

applied as a control to the above chimeric Ii constructs reported by Pond *et al.* (1995), and we found that for neutral tailpieces one may explain ILEV formation using the above hypothesis on electrostatic interactions.

Pond *et al.* (1995) sought to reconstitute large vesicle formation by replacing one or two residues with Asp and obtained two positive (MDQIKRLL and MSDIKRLL) and one neutral (MDDIKRLL) tail. In agreement with our observations, no large vesicles were observed for positively charged tails. More interesting, for the neutral one no large vesicles were formed (Pond *et al.*, 1995), as it can be predicted by our electrostatic hypothesis. This is due to the presence of double (i, i ± 3) electrostatic interactions (between residues 2–5 and 3–6). The results show that Ii-induced vacuolation depends on available negative charges in the Ii N terminus rather than specific amino acids residues.

It was previously reported that Ii constructs with deletions in the luminal domain, which abolished trimerization, did not cause vacuolation (Gedde-Dahl *et al.*, 1997). We did not observe ILEV in cells transfected with chimeric constructs in which the Ii tail was fused to the transmembrane domains of either the transferrin receptor, which is dimeric (Jing and Trowbridge, 1987), or the neuraminidase, which is a tetramer (Bremnes *et al.*, 1994). This suggests that the trimeric conformation of Ii is required for vacuolation. The luminal domain of Ii is sequentially degraded in endosomes, but the tails remain trimeric (Amigorena *et al.*, 1995; Newcomb *et al.*, 1996). Double-staining of ILEV with antibodies against the luminal and the cytoplasmic domains of Ii has demonstrated that the cytoplasmic tails are recognized by antibodies in "late" ILEV after the luminal domain has been degraded (Stang and Bakke, 1997).

It has previously been shown that Ii is retained within the endocytic pathway (Loss and Sant, 1993) where it induces a delayed endocytic transport of both antigens and membrane proteins (Romagnoli *et al.*, 1993; Amigorena *et al.*, 1995; Gorvel *et al.*, 1995). Use of the protease inhibitor leupeptin showed that MHC class II accumulated in late endosomes in association with an Ii-derived fragment, Iip10 (Maric *et al.*, 1994; Amigorena *et al.*, 1995; Brachet *et al.*, 1997). Iip10 harbors an intact cytoplasmic tail and this led to the suggestion that a signal for endosomal retention was present in the cytoplasmic tail of these fragments, which retained MHC class II until Ii processing was complete. It was further suggested that the retention signal likely was constituted of the two Leu-based signals (Maric *et al.*, 1994). However, in a recent study we have shown that expression of Ii_{wt} but not Ii_{D6R} caused endocytosed material destined for the TGN or lysosomes to be retained in endosomes (Gregers *et al.*, unpublished data), suggesting that endosomal retention is not dependent on the two Leu-based signals. Instead, available negative charges in the N terminus of Ii seem to be decisive.

In a previous study, we have reported the structure of a synthetic peptide corresponding to the cytoplasmic tails of Ii_{wt} determined in solution (Motta *et al.*, 1997). At high concentrations, this peptide folds as a trimeric α-helical bundle. Interestingly, these trimers were almost coplanar and antiparallel, arranged in an up-down-up orientation, suggesting that different trimers might interact with each other. This trimeric association, which preserves the secondary structure of the monomer, was shown to be mostly determined by the pattern of polar and hydrophobic residues. NMR spectroscopy was also applied to compare the solution structure of the synthetic peptides corresponding to the cytoplasmic tails of Ii_{wt} and Ii_{D6R}, and they were found to have almost the same overall shape (Motta *et al.*, 1997). When the concentration of the Ii_{wt} tail peptide was increased in methanolic solution, the peptide started to form an aggregate. Interestingly, in similar conditions, the Ii_{D6R} tail peptide did not aggregate, even after being refrigerated for several months. The absence of aggregation correlates with the lack of noticeable differences in NMR spectra at various concentrations (Nordeng, Gregers, Kongsvik, Méresse, Gorvel, Jourdan, Motta, and Bakke, unpublished data), suggesting that internal double-salt bridges (Asp^2-Arg^5 and Asp^3-Arg^6) alter the charge distribution within the tailpiece, thus disfavoring the trimeric association described for the native peptide.

The morphological and structural evidence prompted us to ask for a possible connection between available negative charges in the cytoplasmic tail of Ii, the intrinsic aggregating ability of tails pointing in opposite directions, and the endosomal vacuolation and delayed endocytic trafficking. We have previously suggested that interactions between Ii molecules on separate membranes could promote fusion between endosomes (Motta *et al.*, 1997). In this scenario, membranes of different endosomes are brought together by *trans* interactions between protruding tails. Parton *et al.* (1992) have reported that chemical cross-linking of endosomes in live cells causes vacuolation and partially impaired sorting. Moreover, there are several examples in the literature describing vacuolation in response to increased endosomal fusion (Barbieri *et al.*, 1994; Stenmark *et al.*, 1994). We have searched for a connection between the structural and the morphological data by applying a cell-free fusion assay for endosome membranes containing Ii_{wt} or Ii_{D6R}. Data from these experiments show that in the cell-free system Ii increased endosome fusion by 20%, and it is possible that this could account for the observed effects on the endosomal pathway.

In vitro homotypic fusion between early endosomes has been reported to be almost completely blocked by the PI3-kinase inhibitor wortmannin (Jones and Clague, 1995). In our cell-free assay, wortmannin inhibited fusion between endosomes by ~45%. The reason for the lower efficiency of wortmannin in our assay could be that we used a mixture of early and late endosomes. However, fusion between endosomes from cells expressing Ii_{wt} was inhibited by only ~10% when wortmannin was included in the fusion mixture. Ii_{D6R}, on the other hand, was not able to restore fusion under such conditions. This shows that in the presence of Ii_{wt} endosome fusion is not dependent on the PI3-kinase and suggests that this effect depends on free negative charges within the cytoplasmic tail N terminus.

There are a number of recently discovered proteins that serve to link vesicles with their targets (for reviews, see Pfeffer, 1999; Waters and Pfeffer, 1999). One of these, EEA1 has been shown to bind PI3-phosphate on early endosomes (Mills *et al.*, 1998; Simonsen *et al.*, 1998b; Christoforidis *et al.*, 1999). We observed by live cell microscopy that, although EEA1-GFP rapidly dissociated from endosome membranes upon addition of wortmannin, Ii-induced vacuolation was not sensitive to this treatment. In the presence of Ii_{wt}, endosome fusion was insensitive to wortmannin, whereas NEM

always blocked fusion. This suggests that Ii can complement for PI3-kinase activity in a step before the NEM-sensitive docking of endosomal membranes.

When Ii_{wt}-positive endosomes were mixed with endosomes containing Ii_{D6R}, the wortmannin-induced block of endosome fusion was not restored. One possible explanation for this observation is that Ii_{wt} tails could recruit a cytoplasmic factor involved in homotypic endosome fusion and that Ii_{D6R} fails to recruit such a factor. Another explanation could be that the cytoplasmic tail of Ii_{wt} is not able to form stable antiparallel interactions with tails of Ii_{D6R}. The latter model is supported by NMR calculations showing that electrostatic interactions between the Ii tails depend on available negative charges, which the N-terminal tail of Ii_{D6R} does not provide. Thus, although it is possible that relevant cytoplasmic factors could be recruited specifically by the cytoplasmic tail of Ii, we provide evidence that the aggregating property of the Ii cytoplasmic tail is involved in the regulation of endosome fusion.

The PI3-kinase together with rab5 recruit EEA1 to early endosomal membranes, and it has been suggested that the EEA1 molecules on separate membranes can tether endosomes together by coiled-coil interactions. This is believed to be an early step in the linkage process ultimately causing early endosomes to fuse (for a review, see Pfeffer, 1999; Waters and Pfeffer, 1999). Our data show that in vitro the cytoplasmic tail of Ii can partially complement for endosome tethering by EEA1. Pfeffer (1999) has defined vesicle tethering as involving loose links that extend over distances >25 nm, whereas docking molecules promote rather stable interactions that hold two membranes within a 5- to 10-nm distance. Interactions between antiparallel Ii tails are expected to be quite loose but would not hold membranes with a distance of much more than 5 nm because the tails are quite short (30 amino acids in α helical conformation, including a kink). Hence, Ii does not fall into one or the other category, but we suggest that Ii may serve to stabilize membrane topology in a conformation that favors SNARE interactions and subsequent vesicle fusion.

Ii tails have been found on both early and late endosomes (Stang and Bakke, 1997), and interactions between the tails could therefore cause endosome populations to mix. Consequently, vectorial processes such as transport and proteolysis would be disordered. This theory is supported by recent experimental data showing that high expression of Ii_{wt}, but not Ii_{D6R}, caused endocytosed material destined for the TGN or lysosomes to be retained in endosomes (Gregers *et al.*, unpublished data). Moreover, antigen presentation of an Ii-dependent epitope was shown to be enhanced in cells expressing Ii_{wt} compared with Ii_{D6R}. Even though it remains to be elucidated whether, and under which circumstances, Ii is able to regulate its own intracellular environment in vivo, our data support new aspects of regulation of endocytic transport and endosome size and morphology.

ACKNOWLEDGMENTS

We thank Harald Stenmark and Bjørn Bremnes for helpful discussions. This work was supported by European Community Research Training Networks grant ERBFMRXCT960069 (A.M., F.J., J-P.G, and O.B.). T.F.G and T.W.N were supported by grants from the Norwegian Cancer Society, the Novo Nordisk Foundation, and the Norwegian Research Council.

REFERENCES

Amigorena, S., Webster, P., Drake, J., Newcomb, J., Cresswell, P., and Mellman, I. (1995). Invariant chain cleavage and peptide loading in major histocompatibility complex class II vesicles. J. Exp. Med. *181*, 1729–1741.

Bakke, O., and Dobberstein, B. (1990). MHC class II-associated invariant chain contains a sorting signal for endosomal compartments. Cell *63*, 707–716.

Barbieri, M.A., Li, G., Colombo, M.I., and Stahl, P.D. (1994). Rab5, an early acting endosomal GTPase, supports in vitro endosome fusion without GTP hydrolysis. J. Biol. Chem. *269*, 18720–18722.

Blum, J.S., and Cresswell, P. (1988). Role for intracellular proteases in the processing and transport of class II HLA antigens. Proc. Natl. Acad. Sci. USA *85*, 3975–3979.

Bomsel, M., Parton, R., Kuznetsov, S.A., Schroer, T.A., and Gruenberg, J. (1990). Microtubule- and motor-dependent fusion in vitro between apical and basolateral endocytic vesicles from MDCK cells. Cell *62*, 719–731.

Brachet, V., Raposo, G., Amigorena, S., and Mellman, I. (1997). Ii chain controls the transport of major histocompatibility complex class II molecules to and from lysosomes. J. Cell Biol. *137*, 51–65.

Bremnes, B., Madsen, T., Gedde-Dahl, M., and Bakke, O. (1994). An LI and ML motif in the cytoplasmic tail of the MHC-associated invariant chain mediate rapid internalization. J. Cell Sci. *107*, 2021–2032.

Christoforidis, S., McBride, H.M., Burgoyne, R.D., and Zerial, M. (1999). The Rab5 effector EEA1 is a core component of endosome docking. Nature *397*, 621–625.

Forood, B., Feliciano, E.J., and Nambiar, K.P. (1993). Stabilization of alpha-helical structures in short peptides via end capping. Proc. Natl. Acad. Sci. USA *90*, 838–842.

Gedde-Dahl, M., Freisewinkel, I., Staschewski, M., Schenck, K., Koch, N., and Bakke, O. (1997). Exon 6 is essential for invariant chain trimerization and induction of large endosomal structures. J. Biol. Chem. *272*, 8281–8287.

Germain, R.N. (1994). MHC-dependent antigen processing and peptide presentation: providing ligands for T lymphocyte activation. Cell *76*, 287–299.

Gorvel, J.-P., Chavrier, P., Zerial, M., and Gruenberg, J. (1991). rab5 controls early endosome fusion in vitro. Cell *64*, 915–925.

Gorvel, J.-P., Escola, J.-M., Stang, E., and Bakke, O. (1995). Invariant chain induces a delayed transport from early to late endosomes. J. Biol. Chem. *270*, 2741–2746.

Gruenberg, J., Griffiths, G., and Howell, K.E. (1989). Characterization of the early endosome and putative endocytic carrier vesicles in vivo and with an assay of vesicle fusion in vitro. J. Cell Biol. *108*, 1301–1316.

Huylebroeck, D., Maertens, G., Verhoeyen, M., Lopez, C., Raeymakers, A., Jou, W.M., and Fiers, W. (1988). High-level transient expression of influenza virus proteins from a series of SV40 late and early replacement vectors. Gene *66*, 163–181.

Jing, S.Q., and Trowbridge, I.S. (1987). Identification of the intermolecular disulfide bonds of the human transferrin receptor and its lipid-attachment site. EMBO J. *6*, 327–331.

Jones, A.T., and Clague, M.J. (1995). Phosphatidylinositol 3-kinase activity is required for early endosome fusion. Biochem. J. *311*, 31–34.

Jones, A.T., Mills, I.G., Scheidig, A.J., Alexandrov, K., and Clague, M.J. (1998). Inhibition of endosome fusion by wortmannin persists in the presence of activated rab5. Mol. Biol. Cell *9*, 323–332.

Jorgensen, W.L. (1986). Optimized intermolecular potential functions for liquid alcohols. J. Phys. Chem. *90*, 1276–1284.

Jorgensen, W.L., and Tirado-Rives, J. (1988). The OPLS potential functions for proteins: energy minimizations for crystals of cyclic peptides and crambin. J. Am. Chem. Soc. *110*, 1657–1666.

Koradi, R., Billeter, M., and Wüthrich, K. (1996). Molmol: a program for display and analysis of macromolecular structures. J. Mol. Graphics *14*, 51–55.

Kozak, M. (1987). An analysis of 5′-noncoding sequences from 699 vertebrate messenger RNAs. Nucleic Acids Res. *15*, 8125–8148.

Laemmli, U.K. (1970). Cleavage of structural proteins during the assembly of the head of bacteriophage T4. Nature *227*, 680–685.

Loss, G.E., Jr., and Sant, A.J. (1993). Invariant chain retains MHC class II molecules in the endocytic pathway. J. Immunol. *150*, 3187–3197.

Maric, M.A., Taylor, M.D., and Blum, J.S. (1994). Endosomal aspartic proteinases are required for invariant-chain processing. Proc. Natl. Acad. Sci. USA *91*, 2171–2175.

McBride, H.M., Rybin, V., Murphy, C., Giner, A., Teasdale, R., and Zerial, M. (1999). Oligomeric complexes link Rab5 effectors with NSF and drive membrane fusion via interactions between EEA1 and syntaxin 13. Cell *98*, 377–386.

Mills, I.G., Jones, A.T., and Clague, M.J. (1998). Involvement of the endosomal autoantigen EEA1 in homotypic fusion of early endosomes. Curr. Biol. *8*, 881–884.

Motta, A., Amodeo, P., Fucile, P., Castiglione Morelli, M.A., Bremnes, B., and Bakke, O. (1997). A new triple-stranded alpha-helical bundle in solution: the assembly of the cytosolic tail of MHC-associated invariant chain. Structure *5*, 1453–1464.

Motta, A., Bremnes, B., Morelli, M.A.C., Frank, R.W., Saviano, G., and Bakke, O. (1995). Structure-activity relationship of the leucine-based sorting motifs in the cytosolic tail of the major histocompatibility complex-associated invariant chain. J. Biol. Chem. *270*, 27165–27171.

Newcomb, J.R., Carboy-Newcomb, C., and Cresswell, P. (1996). Trimeric interactions of the invariant chain and its association with major histocompatibility complex class II alphabeta dimers. J. Biol. Chem. *271*, 24249–24256.

Nordeng, T.W., and Bakke, O. (1999). Overexpression of proteins containing tyrosine- or leucine-based sorting signals affects transferrin receptor trafficking. J. Biol. Chem. *274*, 21139–21148.

Nordeng, T.W., Gorvel, J.-P., and Bakke, O. (1998). Intracellular transport of molecules engaged in the presentation of exogenous antigen. Curr. Top. Microbiol. Immunol. *232*, 179–215.

Odorizzi, C.G., Trowbridge, I.S., Xue, L., Hopkins, C.R., Davis, C.D., and Collawn, J.F. (1994). Sorting signals in the MHC class II invariant chain cytoplasmic tail and transmembrane region determine trafficking to an endocytic processing compartment. J. Cell Biol. *126*, 317–330.

Parton, R.G., Schrotz, P., Bucci, C., and Gruenberg, J. (1992). Plasticity of early endosomes. J. Cell Sci. *103*, 335–348.

Pfeffer, S.R. (1999). Transport-vesicle targeting: tethers before SNAREs. Nat. Cell Biol. *1*, E17–22.

Pieters, J., Bakke, O., and Dobberstein, B. (1993). The MHC class II associated invariant chain contains two endosomal targeting signals within its cytoplasmic tail. J. Cell Sci. *106*, 831–846.

Pond, L., Kuhn, L.A., Teyton, L., Schutze, M.P., Tainer, J.A., Jackson, M.R., and Peterson, P.A. (1995). A role for acidic residues in di-leucine motif-based targeting to the endocytic pathway. J. Biol. Chem. *270*, 19989–19997.

Quaranta, V., Majdic, O., Stingl, G., Liszka, K., Honigsmann, H., and Knapp, W. (1984). A human Ia cytoplasmic determinant located on multiple forms of invariant chain (gamma, gamma2, gamma3). J. Immunol. *132*, 1900–1905.

Romagnoli, P., Layet, C., Yewdell, J., Bakke, O., and Germain, R.N. (1993). Relationship between invariant chain expression and major histocompatibility complex class II transport into early and late endocytic compartments. J. Exp. Med. *177*, 583–596.

Ryckaert, J.P., Ciccotti, G., and Berendsen, H.J.C. (1977). Numerical integration of the Cartesian equations of motions of a system with constraints: molecular dynamics of *n*-alcanes. J. Comp. Phys. *23*, 327–341.

Schutze, M.-P., Peterson, P.A., and Jackson, M.R. (1994). An N-terminal double-arginine motif maintains type II membrane proteins in the endoplasmic reticulum. EMBO J. *13*, 1696–1705.

Simonsen, A., Bremnes, B., Nordeng, T.W., and Bakke, O. (1998a). The leucine-based motif (DDQxxLI) is recognized both for internalization and basolateral sorting of invariant chain in MDCK cells. Eur. J. Cell Biol. *76*, 25–32.

Simonsen, A., Lippe, R., Christoforidis, S., Gaullier, J.M., Brech, A., Callaghan, J., Toh, B.H., Murphy, C., Zerial, M., and Stenmark, H. (1998b). EEA1 links PI(3)K function to Rab5 regulation of endosome fusion. Nature *394*, 494–498.

Stang, E., and Bakke, O. (1997). MHC class II associated invariant chain induced enlarged endosomal structures: a morphological study. Exp. Cell Res. *235*, 79–82.

Stenmark, H., Parton, R.G., Steele-Mortimer, O., Lütcke, A., Gruenberg, J., and Zerial, M. (1994). Inhibition of rab5 GTPase activity stimulates membrane fusion in endocytosis. EMBO J. *13*, 1287–1296.

Waters, M.G., and Pfeffer, S.R. (1999). Membrane tethering in intracellular transport. Curr. Opin. Cell Biol. *11*, 453–459.

Weiner, S.J., Kollman, P.A., Case, D.A., Chandra Singh, U., Ghio, C., Alagona, G., Profeta, S., and Weiner, P.K. (1984). A new force field for molecular mechanical simulation of nucleic acids and proteins. J. Am. Chem. Soc. *106*, 765–784.

Wigler, M., Pellicer, A., Silverstein, S., Axel, R., Urlaub, G., and Chasin, L. (1979). DNA-mediated transfer of the adenine phosphoribosyltransferase locus into mammalian cells. Proc. Natl. Acad. Sci. USA *76*, 1373–1376.

Wraight, C.J., van Endert, P., Moller, P., Lipp, J., Ling, N.R., MacLennan, I.C., Koch, N., and Moldenhauer, G. (1990). Human major histocompatibility complex class II invariant chain is expressed on the cell surface. J. Biol. Chem. *265*, 5787–5792.